Pure appl. geophys. 159 (2002) 2113–2131
0033–4553/02/092113–19 $ 1.50 + 0.20/0

Pure and Applied Geophysics

The Influence of 3-D Structure on the Propagation of Seismic Waves Away from Earthquakes

BRIAN L. N. KENNETT[1] and TAKASHI FURUMURA[2]

Abstract — The seismic records from significant earthquakes are profoundly affected by 3-D variations in crustal structure both in the source zone itself and in propagation to some distance. Even in structurally complex zones such as Japan and Mexico relatively coherent arrivals are found associated with different classes of propagation paths. The presence of strong lateral variations can disrupt the arrivals, and impose significant variations in propagation characteristics for different directions from the source as illustrated by observations for the 1995 Kobe and 2000 Tottori-ken Seibu earthquakes in western Japan. Such effects can be modelled in 3 dimensions using a hybrid scheme with a pseudospectral representation for horizontal coordinates and finite differences in depth. This arrangement improves parallel implementation by minimising communication costs. For a realistic 3-D model for the structure in western Japan the 3-D simulations to frequencies close to 1 Hz provide a good representation of the observations from subduction zones events such as the 1946 Nankai earthquake and the 2000 Tottori-ken Seibu earthquake. The model can therefore be used to investigate the pattern of ground motion expected for future events e.g., in current seismic gaps.

Key words: 3-D numerical simulation, pseudospectral method, finite differences, regional phases, ground motion patterns.

Introduction

Although the seismic source dictates a large part of the character of the seismic disturbances, the interaction of the radiation from the source with 3-D structure in tectonic regions can play an important role in the patterns of observed ground motion. The influence of structure in the immediate neighbourhood of the source can significantly impact the focussing and defocussing of seismic energy; 3-D numerical simulations suggest that such local effects dictate the position of the narrow zone of damage for the 1995 Kobe earthquake (KAWASE, 1996; FURUMURA and KOKETSU, 1998). Such 3-D simulations for the local wavefield have also been used in other scenarios such as the estimation of site amplification effect in the Los Angeles basin (e.g., OLSEN and ARCHULETA, 1996; WALD and GRAVES, 1998; OLSEN, 2000).

[1] Research School of Earth Sciences, Australian National University, Canberra ACT 0200, Australia. E-mail: brian@rses.anu.edu.au

[2] Earthquake Research Institute, University of Tokyo, 1-1-1 Yayoi, Bunkyo-Ku, Tokyo 113-0032, Japan. E-mail: furumura@eri.u-tokyo.ac.jp

As the seismic waves spread away from the source, the different components of the wavefield interact with crustal and mantle structure in a variety of ways. In regions with subduction, these effects can lead to quite complex behaviour in the distance range out to a few hundred kilometres from the source, for both observations and 3-D simulations of subduction events in Mexico (FURUMURA and KENNETT, 1998). As we shall see, the presence of the Philippine Sea plate and the 3-D topography on crustal interfaces can lead to significant focussing of crust-mantle reflections for events in the Nankai trough in Japan, with consequent enhanced intensity at the surface. Even where the events lie above the subduction zone, the complex 3-D structure in the crust overlying the zone can significantly modify the wavefield.

Although the general properties of the regional seismic wavefield are well known (see e.g., KENNETT, 1989), there have been few simulations of the effect of 3-D structure because it is necessary to follow relatively high frequency waves to a large number of wavelengths from the source. Even with efficient numerical schemes such as the pseudospectral method, there is a large computational burden. FURUMURA and KENNETT (1998) performed both 2-D and 3-D modelling for subduction events in Mexico, and included a more complex source with 3 subevents to improve the description of the great 1985 Michoacan earthquake, and particularly the representation of the destructive effects in Mexico City, over 350 km from the epicentre.

In this paper we consider observations and simulations for seismic events in western Japan, where propagation of guided wave energy in the crust (*Pg*, *Lg*) is quite efficient (FURUMURA and KENNETT, 1998). Differences in the character of the regional wavefield lead to asymmetry in the intensity and ground velocity produced by the 1995 Kobe and the 2000 Tottori-ken Seibu earthquakes with amplitudes sustained at longer distances in the west. With the aid of a full 3-D model for the structure in western Japan, including the crust and subduction zone, it is possible to simulate the effects of earthquakes in different locations. Even a simple point-source model for the 1946 Nankai earthquake produces banding in intensity associated with multiple crust-mantle reflections that match well with the observed intensity patterns for the event. A more complex source model is needed for the 2000 Tottori-ken Seibu earthquake to provide an appropriate balance between high and low frequency components of the wavefield.

Regional Phase Propagation in Japan

SHIMA (1962) recognised differences at Matsushiro observatory in the velocity and clarity of the *Lg* phase from the southwest and northeast. However, subsequently little attention has been paid to the detailed character of the regional wavefield within Japan, although local models have been developed for location purposes. The recent dramatic increase in the density of high-quality seismic data in

Japan means that it is now possible to undertake a detailed tomographic study of the efficiency of crustal *S*-wave propagation (FURUMURA and KENNETT, 2001).

The cooperative efforts of Japanese Universities have established a remarkable data set from the stations of the *J*-array coordinated by the Earthquake Research Institute, University of Tokyo. Recent seismic events of magnitude 5 and above have been recorded by up to 200 stations. The assembly of the data from 50 events has provided over 8000 paths sampling the region, which allows the characterisation of the spatial variation in regional phase propagation (FURUMURA and KENNETT, 2001). The amplitude ratios of *Lg* and *Sn* phases provide a convenient measure of the nature of the regional *S*-wave field. This measure has the merit of being both relatively insensitive to local site conditions and also being easy to automate.

Figure 1 illustrates the transmissivity of *Lg* derived by a tomographic inversion from the path samples. A significant area exists in western Japan (part of Kyushu, Shikoku, western Honshu) for which *Lg*-wave propagation is efficient. For events within this region, *Lg* would normally be the dominant phase on the seismic record and guided *S*-wave energy in the crust would represent the major mode of energy from the source to distances beyond 150 km. Propagation to the west would be expected to be more efficient than to the east.

Recent Large Earthquakes in Western Japan

Two large destructive earthquakes have occurred in western Japan in recent years. The 1995 Hyogo-ken Nanbu (Kobe) earthquake (M_w 6.9) inflicted major damage in the city of Kobe and strong shaking distributed over a large region. Following this event a major upgrade of strong ground motion recording was made and there is now a high density of digital accelerometers across Japan. The 2000 Tottori-ken Seibu event (M_w 6.6) was well recorded by the new networks and this allows a good assessment of the wavefield from close to the source outwards.

For both the Kobe and the Tottori-ken Seibu events the estimates of the magnitude (M_j) provided by the Japan Meteorological Agency (JMA) are significantly larger than the moment magnitude M_w. The difference is particularly marked for the 2000 event for which the M_j value is 7.3 as compared to M_w 6.6. This discrepancy appears to be due to the dominance of crustal energy whose distance dependence is very different from the assumptions in the standard M_j estimate (FURUMURA and KENNETT, 2001). The differences in the efficiency of propagation between the west and east of the earthquakes is reflected in the patterns of seismic ground motion. For the 1995 Kobe event, the contours of seismic intensity are asymmetric (Fig. 2) and higher intensity is generally encountered to the west for comparable distances from the source. The reason can be seen in a velocity record sections (Fig. 3) derived from JMA accelerometer stations. The dominant energy is in *Lg* and the amplitude is maintained to longer distances in the west.

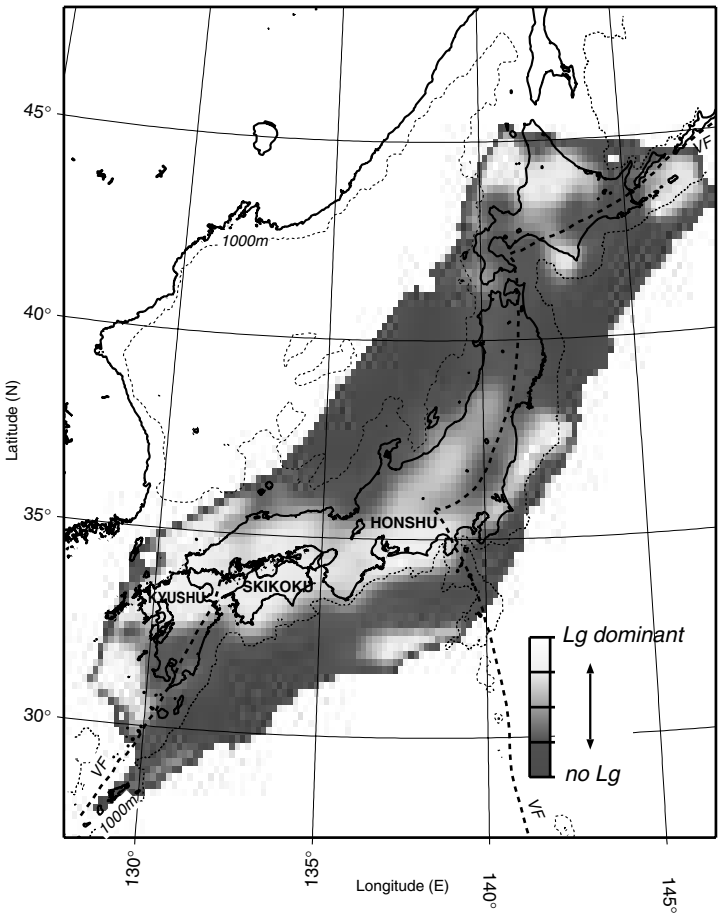

Figure 1
Summary map of the variations in *Lg*/*Sn* ratio for propagation paths through different parts of Japan.

For the 2000 Tottori-ken Seibu earthquake, extensive digital strong-ground-motion data is available from KiKnet and K-net operated by the Japanese National Research Institute for Earth Sciences and Disaster Prevention. We are therefore able to obtain a quantitative assessment of the peak ground velocity produced by the event (Fig. 4) which again shows extension of contours to the west. The records for this shallow event (Fig. 5) at the stations marked with solid squares in Figure 4 indicate that the strong *Lg* phase is reinforced in the west by the presence of strong fundamental mode Rayleigh waves (*Rg*) and a similar situation occurs for Love waves on the tangential component (*LQ*). These lower frequency fundamental mode waves follow large amplitude *Lg* waves and are even more pronounced in displacement, from which the JMA magnitude is derived.

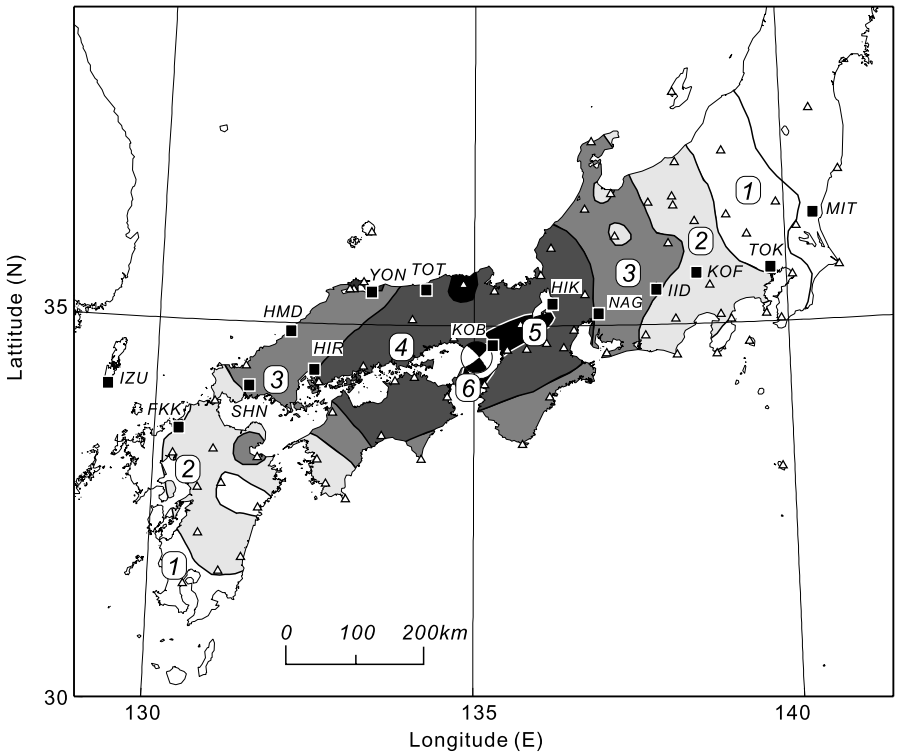

Figure 2
The pattern of intensity for the seven point Japanese scale from the 1995 Kobe earthquake showing elongation of intensity contours to the west of the event. Records from the named stations are included in the sections shown in Figure 3.

The peak velocity pattern in Figure 4 also indicates the way that local conditions influence the ground velocities. The sedimentary basins around Osaka and Nagoya produce local amplification and extend the 2 cm/s and 1 cm/s contours. This reminds us that when we approach seismic modelling we must have a means of introducing local structural variations. The influence of local sediments can be seen in the eastern portion of the record section for the station FKIH05 near Fukui (the third trace from the right) in the form of an extended train of higher frequency waves on the horizontal components.

Modelling the Regional Seismic Wavefield in 3-D

Such observations of the regional wavefield make it clear that it is important to include 3-D effects in any modelling. For western Japan we must include both crustal variability and the complex configuration of the underlying Philippine Sea

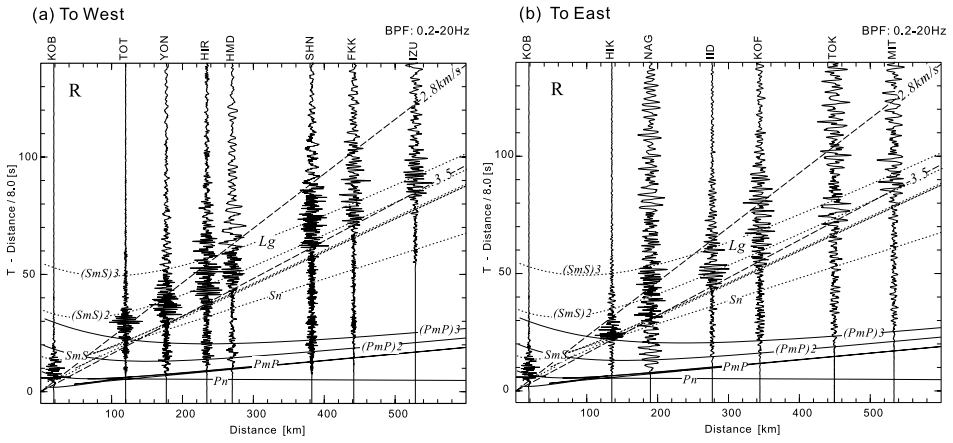

Figure 3
Record sections of ground velocity for the 1995 Kobe earthquake derived from JMA accelerometers showing the strong propagation of *Lg* waves to the west. The horizontal component records have been rotated to lie along the path from the epicentre to the station. The records are normalised to peak amplitude. The traveltime curves for a stratified reference model are superimposed on the records to provide a guide to the physical character of the arrivals.

plate. Subduction along the Nankai trough is responsible for very large earthquakes, as e.g., the 1946 magnitude 8.0 event, which have high destructive potential.

The work of FURUMURA and KENNETT (1998) on the simulation of regional wave propagation from the Guerrero region of Mexico indicates the important role which can be played by a shallowly dipping subduction zone. With the shallow dip there is a large contact area of the subducted plate with the crust and this contact zone can act as a secondary radiator injecting energy into the crustal waveguide to reinforce the radiation coming directly from the source. When, as in Mexico, there is also a significant contrast at a mid-crustal discontinuity (Conrad) there is the possibility of concentration of energy in the upper crust. The effect is to enhance the surface expression of the crustally ducted energy in e.g., the *Lg* phase. The substantial damage in Mexico city in 1985, over 350 km away from the source of the M_w 8.5 earthquake, arises from the enhanced *S* wavefield at the surface interacting with the low velocity sediments of the valley of Mexico.

Our 3-D model for western Japan builds on a variety of data sources for the configuration of the Moho and Conrad discontinuities (ZHAO *et al.*, 1992), velocity structure from receiver function analysis (SHIBUTANI *et al.*, 2000), reflection experiments (YOSHII *et al.*, 1974; HASHIZUME *et al.*, 1981) and *P*- and *S*-wave traveltime tomography (ZHAO and HASEGAWA, 1993). We have assigned anelastic attenuation (Q) factors of 100 for the upper crust, 400 for the lower crust, 600 in the upper mantle and 800 for the Philippine Sea plate.

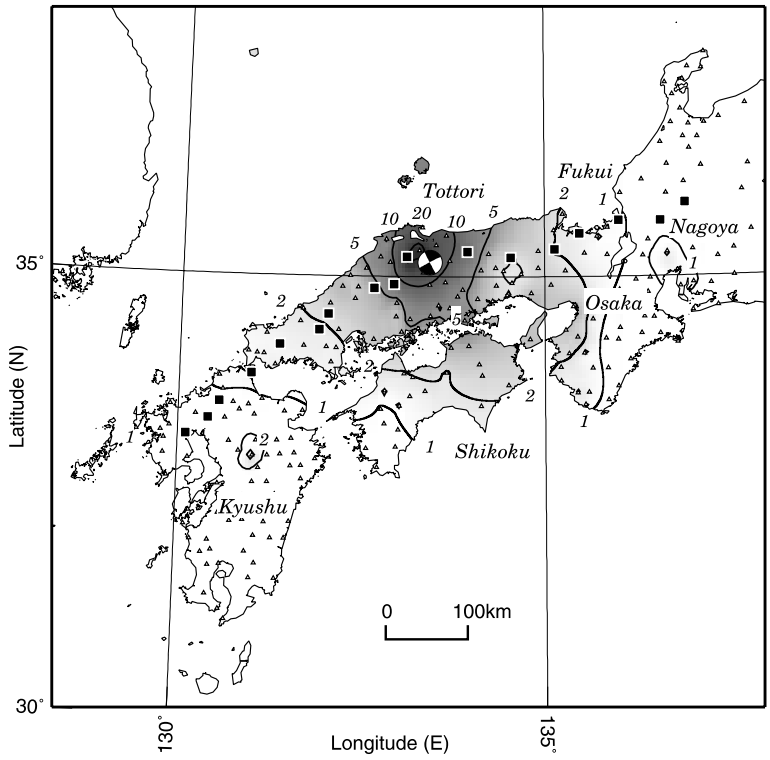

Figure 4
Peak ground velocity in cm/s for the 2000 Tottori-ken Seibu earthquake derived from the digital records of strong-ground motion stations indicated by triangles. Records from the stations shown with solid squares are displayed in figure 5.

A region of 820×410 km in horizontal dimensions and 125 km in depth is used with a hybrid wave simulation procedure based on a pseudospectral formulation in the horizontal coordinates and a conventional fourth-order finite difference scheme in depth. The mesh is $512 \times 256 \times 160$ points with a horizontal mesh increment of 1.6 km and a vertical increment of 0.8 km. The advantage of such a hybrid PSM/FDM approach is that interprocessor communication overheads can be minimised in a parallel implementation (FURUMURA *et al.*, 2002). The PSM/FDM scheme uses a finer mesh for the z coordinate, whereas the FDM is used for calculating vertical derivatives, therefore a higher resolution of 3-D structure can be achieved in the vertical direction.

The configuration of the study region in western Japan and the contours of the subduction zones are shown in Figure 6(a), and a projective view of the major interfaces is illustrated in Figure 6(b). Relative to the scale of the model, topography is low and we have not attempted to model the shallow water in the Inland Sea. Details of the model parameters are shown in Table 1; in order to carry out wave

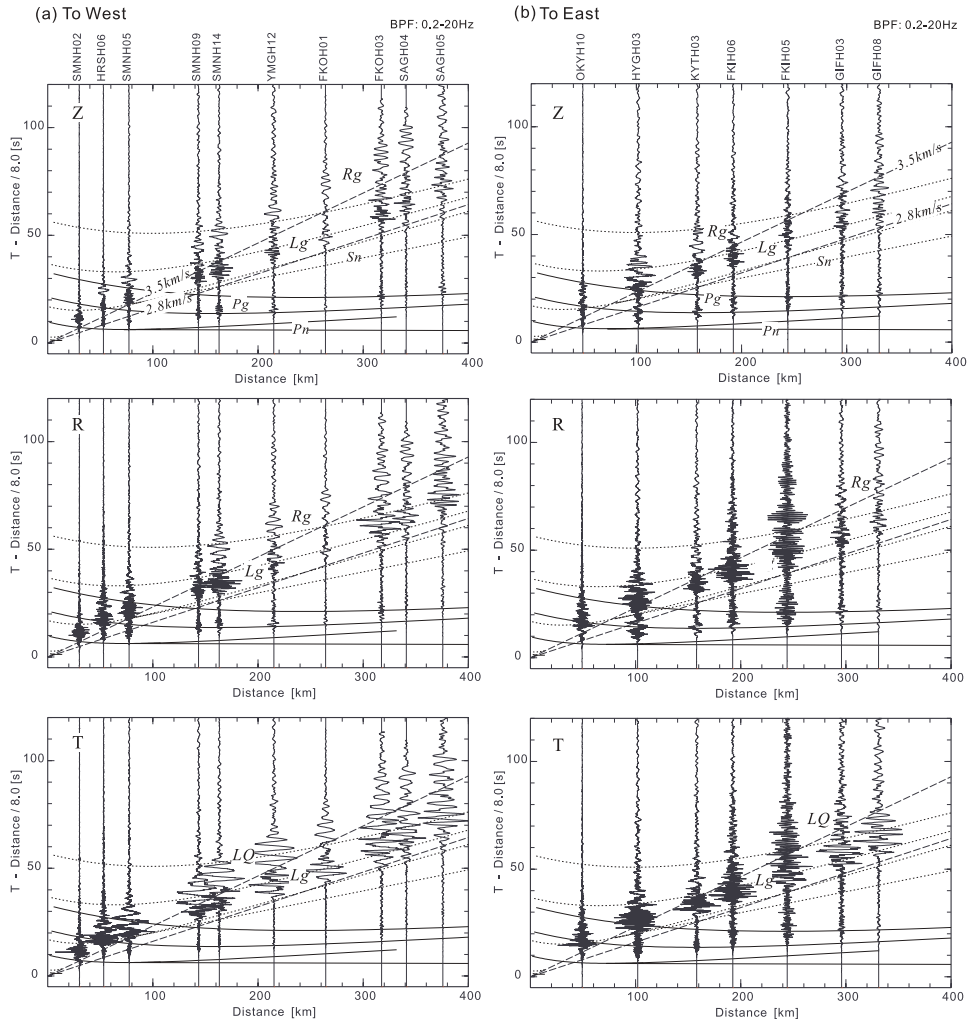

Figure 5
Three-component record sections of ground velocity from the 2000 Tottori-ken Seibu earthquake derived from KiKnet stations. The horizontal components have been rotated to lie along (R) and perpendicular to (T) the path to the epicentre. Strong fundamental mode Rayleigh (*Rg*) and Love (*LQ*) waves are seen to the west accompanying *Lg*.

propagation simulations in such a complex model, compromises are necessary particularly for the representation of shallow structure. The water layer is excluded from the model and is replaced by the surficial layers 1 and 2. For most of the region the water depth is less than the grid spacing. Only along the edges of the structural model are oceanic depths approaching 4 km. Attention is focussed on the Japanese Islands so the influence of deeper water is minimised. We also exclude surface

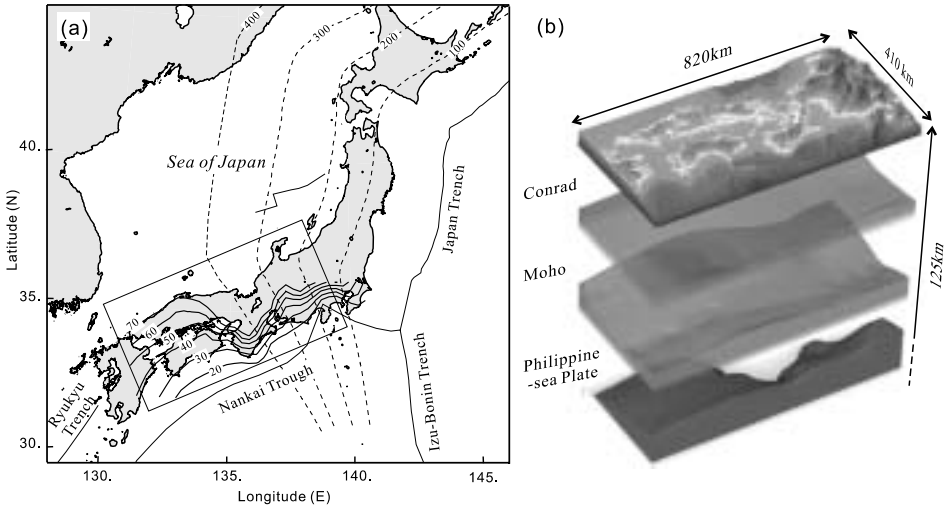

Figure 6
Structural model for western Japan used in 3-D wavefield calculations. (a) Outline of study area and contours of depth to the subduction zones, the Philippine plate is shown with solid lines and the Pacific plate with dashed lines. (b) Detail of 3-D model showing the configuration of the Conrad (mid-crustal) discontinuity, the Moho and the Philippine plate. The surface topography is shown for geographic reference in the wavefield simulations.

topography (less than 2 km across the region) and the details of sedimentary basins from the 3-D calculations, so that the simulations are for a level competent surface.

We consider here a simulation of a subduction zone event (1946 Nankai earthquake) and a shallow crustal event (2000 Tottori-ken Seibu earthquake) using relatively simple source models. Our main purpose is to examine the way in which the interaction of the source radiation with the complex 3-D structure affects the relative significance of the different components of the seismic wavefield.

The minimum S wave velocity for the superficial layer in the 3-D model is 3.0 km/s; so that the PSM/FDM hybrid simulation can accurately treat seismic wave propagation in the frequency band below 0.83 Hz with a sampling of 2.25 grid points per shortest wavelength in the horizontal coordinates and 4.5 grid points in the vertical coordinate.

In Figure 7 we show a display of the horizontal ground velocity at the surface produced from the 3-D propagation model for the Nankai earthquake, represented as a shallow angle thrust fault at 20 km depth on the upper edge of the subduction zone. We have used a characteristic period of 1.2 s for the source time function. The peak ground velocity from the 3-D calculations is displayed in Figure 8 and the seismograms along two profiles, (a) to western Japan and (b) to central Japan, are illustrated in Figure 9.

The first snapshot of horizontal ground velocity at 17.5 s after source initiation (Fig. 7a) shows the P wavefront as an outer rampart to the larger amplitude S

Table 1

Model parameters used in the 3D simulation

	V_p (km s^{-1})	V_s (km s^{-1})	ρ (Mg m^{-3})	Q_s	Thickness (km)
		Japanese Islands			
Layer 1	5.4	3.0	2.3	100	2.0
Layer 2	5.7	3.2	2.4	100	3.0
Upper Crust	6.1	3.5	2.6	200	2.8–15.7
Lower Crust	6.6	3.8	2.8	400	5.8–23.6
Upper Mantle	8.0	4.6	3.0	800	–
		Philippine Sea Plate*			
Oceanic Crust	5.5–7.6	3.1–4.2	2.1–2.9	100	4.0
Oceanic Basalt	6.7–7.6	3.7–4.2	2.8–2.9	150	4.0
Oceanic Mantle	8.1–8.5	4.7–4.9	3.1–3.2	1000	32.0

*Below 40 km depth the velocities in the oceanic crustal layers in the subducting plate are reduced. The contrast with the oceanic mantle decreases gradually with increasing depth.

disturbance on which the effect of the source radiation pattern is quite clear. In the snapshot at 52.5 s (Fig. 7b) the *P* waves are still visible but have separated into a group of distinct arrivals, which are followed by the *Sn* arrivals and then the main amplitude of the *S* waves which is beginning to separate into components with slightly different group velocities. The 3-D structure has begun to impose its own modulation of the *S*-wave amplitudes in addition to the initial pattern imposed by the source. In the frame at 87.5 s after source initiation (Fig. 7c), the *S* waves have reached about 300 km from the source and there are two distinct wave groups corresponding to different multiple *S* reflections from the crust-mantle boundary.

The peak ground velocity patterns in Fig. 8 indicate the presence of noticeable focussing of ground motion induced by the propagation processes. Figure 8 presents a comparison of the ground motion pattern for the full model including the Philippine Sea plate (Fig. 8A) with the corresponding results in Figure 8B without the presence of a subduction zone. The influence of the subduction zone near the source is significant and modulates the main pattern imposed by the crustal structure seen in Figure 8B. Along profile (b) to the northeast in Figure 8A we see three distinct peaks in the peak ground velocity which we can relate to successive *S*-wave reflections from the crust-mantle boundary (with an intermediate surface reflection). These strong bursts of energy are very clearly seen in the seismograms in Figure 9. Similar effects are seen for profile (a), however the energy distribution is more spread along the branches and exhibits more variation with distance. The *Pn* phase is quite distinct on profile (a), but is weak on profile (b) because of the position of the profile relative to the focal mechanism. There is no clear *Pg* arrival, but instead substantial surface reflected *P* energy is found from distances between 100 and 200 km at a reduced time of 12 s. Comparison of the results for profiles (a) and (b) shows that the effect of 3-D structure imposes noticeable differences, but that in both there is a clear

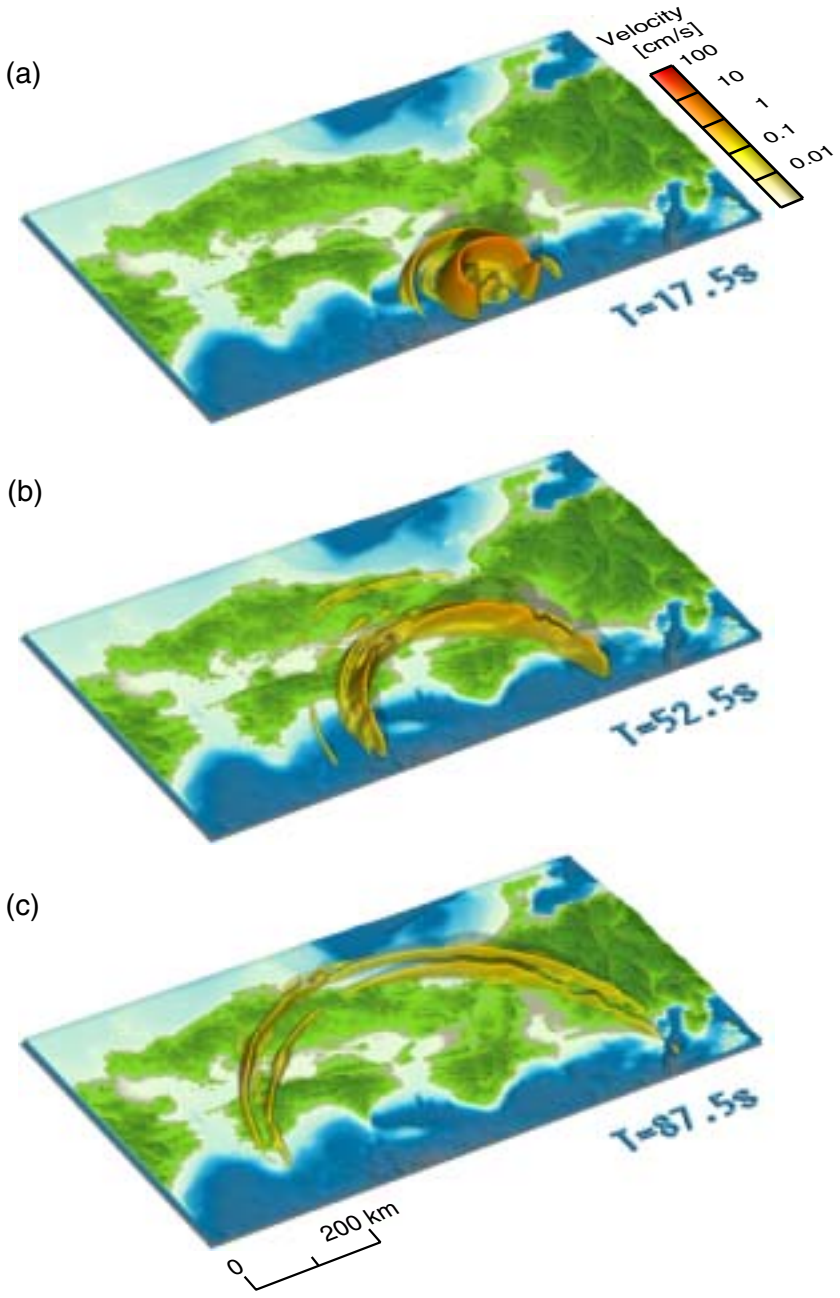

Figure 7
Snapshots of horizontal ground motion from a 3-D simulation of wave propagation from a point source in the Nankai region.

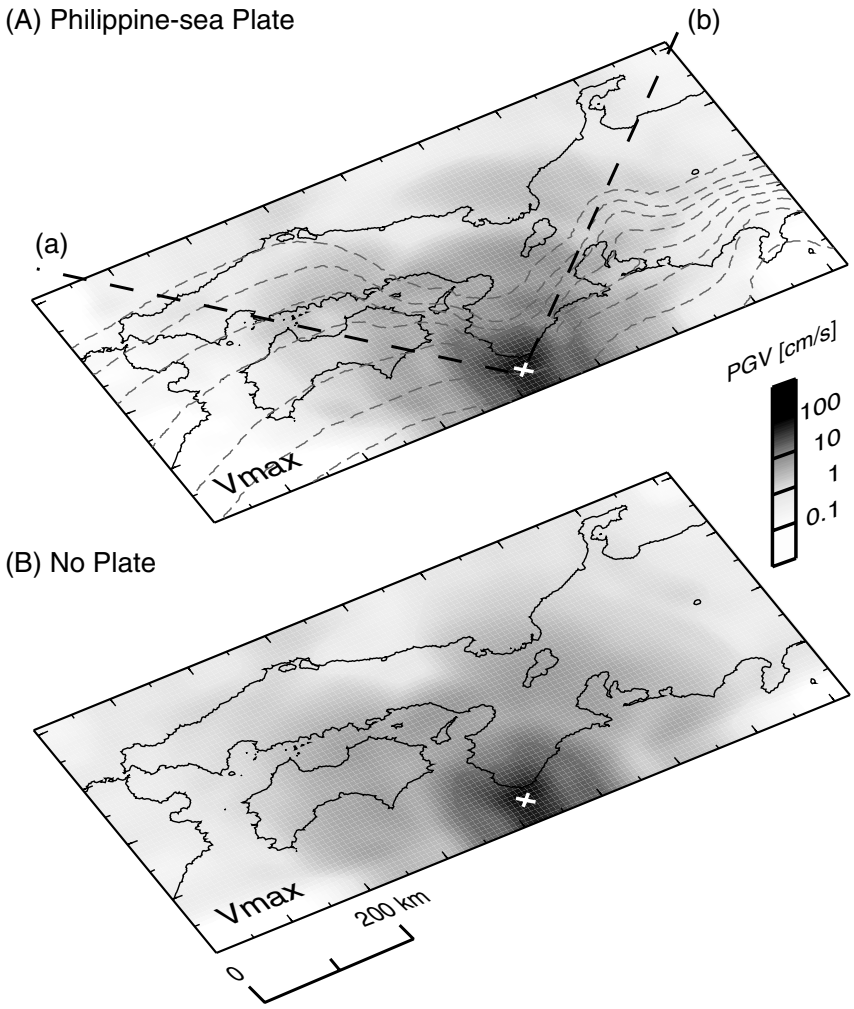

Figure 8
Peak ground velocity derived from the 3-D simulation of the point Nankai event, (A) including the Philippine Sea plate as indicated in Figure 6, the contours of the upper surface of the plate as shown by dashed lines, (B) with no plate structure.

group of energy which is travelling through the crust supported by multiple reflections at the surface and the crust-mantle boundary.

The large amplitudes associated with the individual $(SmS)_n$ reflections would have the potential for imposing marked local variation in seismic ground motion at even 200 km from a great earthquake like the 1946 Nankai event. The intensity pattern for the Nankai event, which had a very large rupture area, exhibits banding with higher intensities than the surroundings in the distance range where we would expect multiple *SmS* (Fig. 10). There is a good correspondence with the features of the point

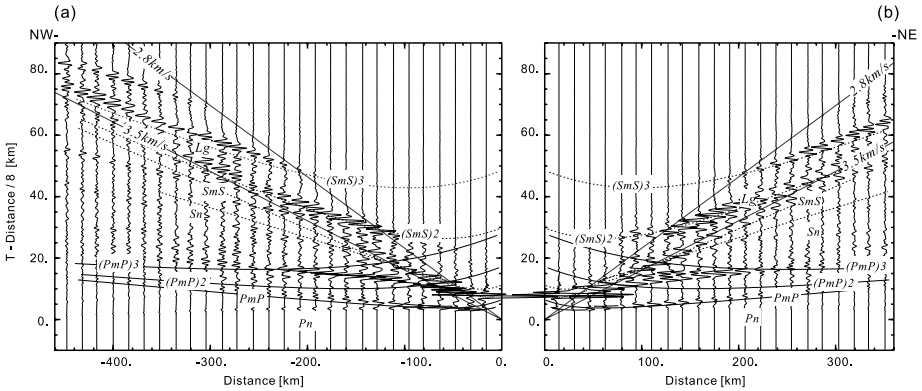

Figure 9
Radial component record sections from the 3-D simulation of the point Nankai event. The traveltime curves for a stratified reference model are superimposed on the records to provide a guide to the physical character of the arrivals.

source simulation eastward from 134°E. The higher ground velocities near Lake Biwa and lower ground velocities along a stretch of the Japan Sea coast match well with the simulation in Figure 8A. The high level of ground velocities in Shikoku and Kyushu are related to the western extension of the faulting in the 1946 event which cannot be simulated with the simple point source.

For our Nankai simulation, the subduction zone dip for the Philippine Sea plate in the region of the source is not very shallow and the trench lies further away from Shikoku than in Mexico. As a result secondary reinforcement from the slab edge is not a major component in this case, but as we see from Figure 8, the presence of the slab near the source has a noticeable effect on the wavefield. Such slab influences could be expected to be even more significant for plate-margin events to the west off Shikoku where the dip of the slab is shallower.

We can contrast this subduction zone event with a shallower earthquake that occurred well away from the plate boundary. The 2000 Tottori-ken Seibu earthquake is a strike-slip event with a hypocentre at 11 km. The fault slip model for the Tottori-ken Seibu earthquake shows one small asperity at 10 km northwest of the hypocentre and a depth of 13.5 km, and one large and 20 km long asperity at 5 km deep crossing the epicenter from northwest to southwest (SEKIGUCHI and IWATA, 2000; YAGI and KIKUCHI, 2000).

As we have seen in Figure 5, the records for this event show clear fundamental mode Rayleigh waves (*Rg*), particularly to the west of the event. These waves are only significant for shallow excitation. We have built a moderately complex model for this event by the superposition of four subevents with the same strike-slip configuration. The fault rupture propagates bilaterally to the north and the south from the hypocentre with a rupture velocity of 2.5 km/s. The main event with 48% of

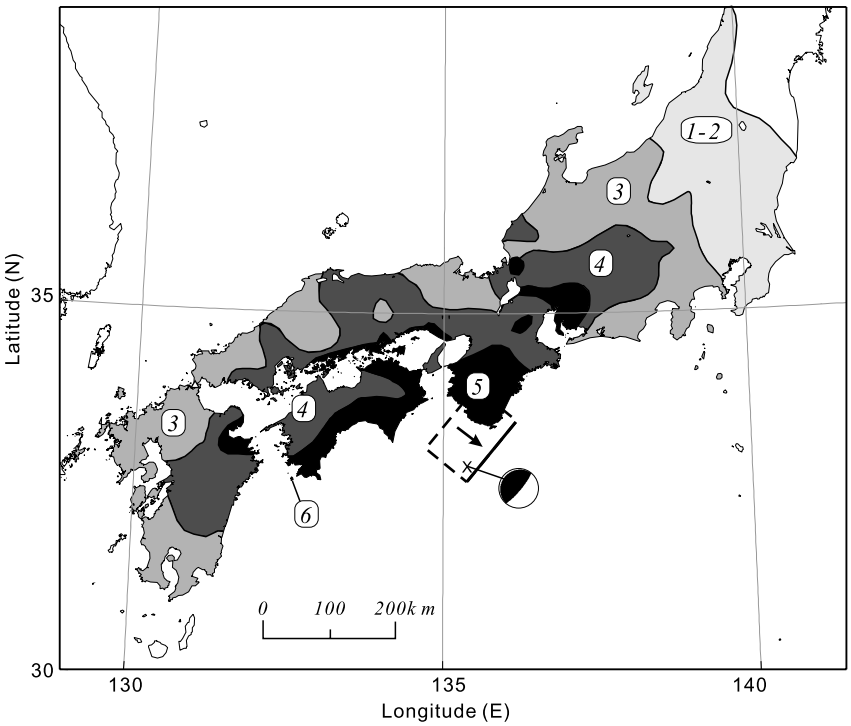

Figure 10
The pattern of seismic intensity of Japanese scale from the 1946 Nankai earthquake. The dashed line outlines the slip area and the arrow indicates the slip direction for the fault model of KANAMORI (1972).

the moment of the M_w 6.6 earthquake is placed at 7.7 km northeast of epicenter and 9.1 km deep with a dominant period of 3.6 s, after which three subevents are introduced to account for the remaining moment release. The first subevent lies 10 km to the northwest of the hypocentre at a depth of 13.5 km with 10% of the moment and a 1.2 s dominant period, the second and larger subevent is above the hypocentre at 4.5 km depth with 32% of the moment and 2.4 s period, and the third event is at 7.1 km northwest of the hypocentre at 4.5 km depth with 10% of the moment. The seismic moment and predominant period for each subevent is determined from the total slip and the size of the asperities in the fault models.

Figure 11 presents a set of snapshots of the horizontal ground velocity in the 3-D simulation for the complex source model of the Tottori-ken event. The dominant strike slip radiation pattern is clear in both the *P* and *S* radiation in the earlier frames (Fig. 11a). As the waves propagate further from the source, the effects of the 3-D model become more apparent and impose their own modulation (Fig. 11c). The *S* arrivals in Figure 11 are more concentrated than in Figure 7 because the thinner crust beneath the northern coast of Honshu leads to overlap of multiple crustal reflections.

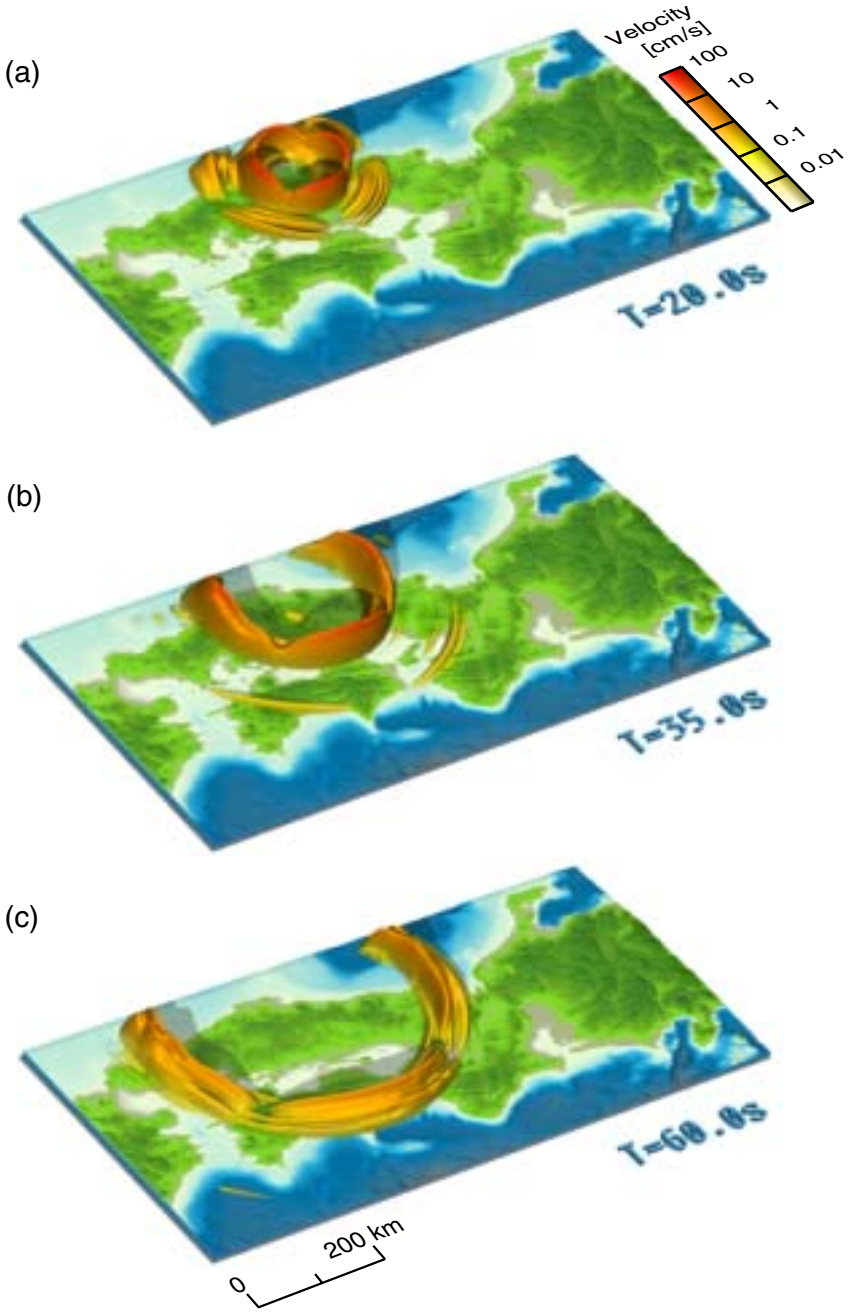

Figure 11
Snapshots of horizontal ground velocity for a 3-D simulation of propagation from the 2000 Tottori-ken Seibu earthquake.

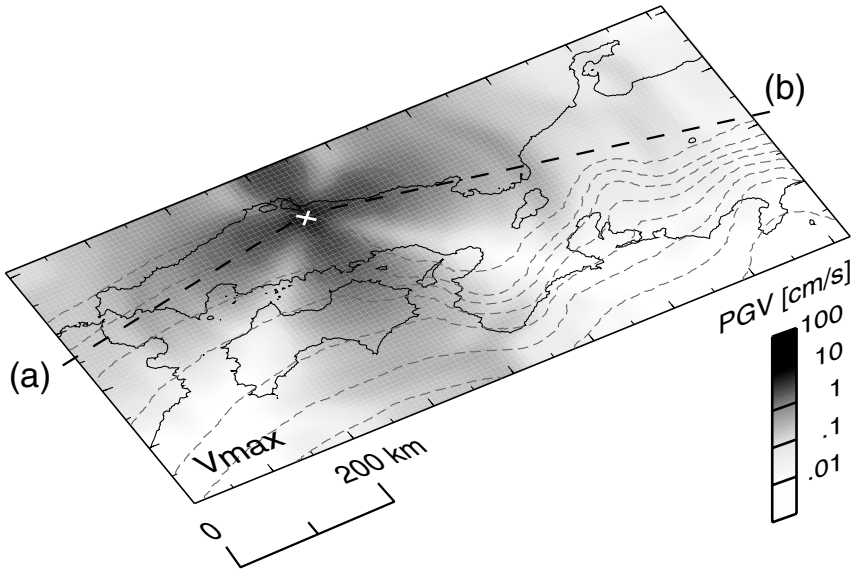

Figure 12
Peak ground velocity derived from 3-D simulation of the 2000 Tottori-ken Seibu earthquake with a complex source.

The *S* waves are closely followed by the fundamental mode surface waves which are associated with the largest energy in the snapshots of Figure 11. The peak ground velocity pattern for the 3-D simulation is shown in Figure 12, indicating the way in which the *S* radiation pattern and structural effects interact.

In Figure 13 we display record sections of the horizontal component seismograms for the 3-D model of western Japan with the complex source. The line of the seismogram profiles lies close to the observations shown in Figure 5. As in the observed field *Lg* is the dominant phase and now has a concentration of amplitude associated with the overlap of successive multiple *S* reflections. Our composite source model generates longer-period seismic waves with dominant period around 1 to 4 sec and the large slip component at shallow depth provides a rather good simulation of the excitation of significant *Rg* energy and correctly predicts higher amplitudes to the west. The excitation of fundamental mode Love waves on the tangential component is also reasonably well simulated.

Discussion — Future Goals for Modelling

These two examples illustrate that we are able to use the 3-D model as a simulation of the general characteristics of observed events. The match to observations is improved if we can use a specific source model for an event. Thus,

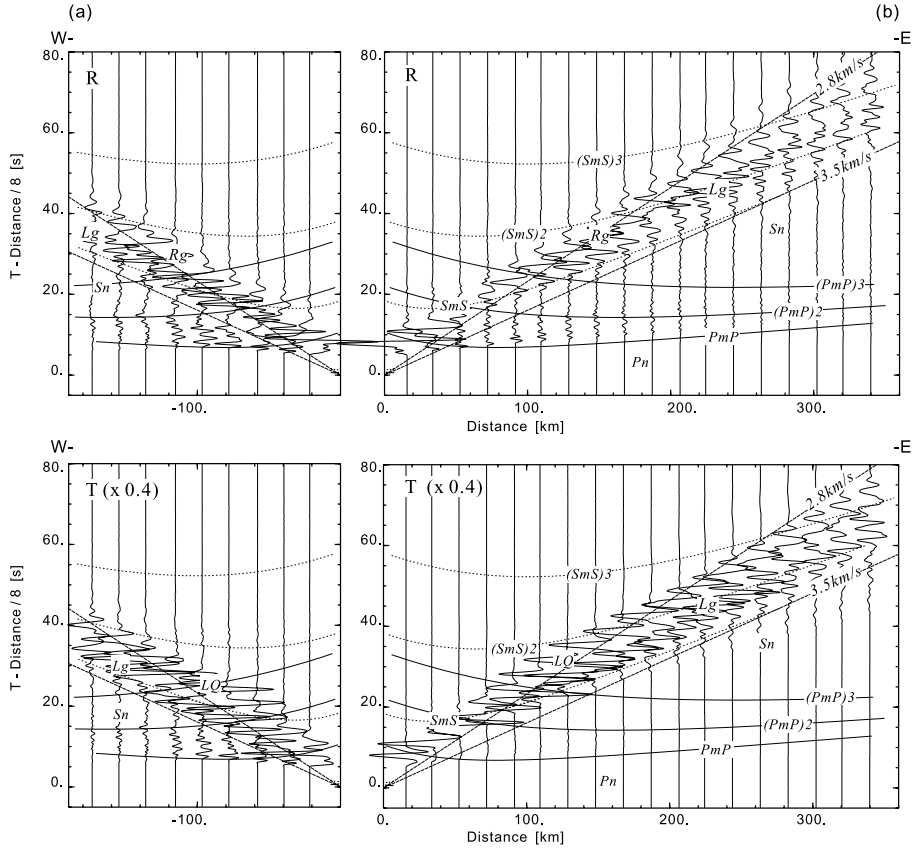

Figure 13
Horizontal component record sections from the 3-D simulation of wave propagation from the 2000 Tottori-ken Seibu earthquake. The traveltime curves for a stratified reference model are superimposed on the records to provide a guide to the physical character of the arrivals.

we could account for the fundamental mode surface waves of the Tottori-ken Seibu earthquake by including the component of shallow slip. The 3-D structural model can therefore be used with the hybrid PSM/FDM method to provide simulations of the ground motion for possible events in the region. Modelling of the propagation conditions for future events can be very helpful for assessing their potential impact. This class of simulation is likely to be of considerable value for events in the Nankai trough, which has a history of great destructive earthquakes but which has not been active in the past 50 years.

The present generation of 3-D modelling codes such as the hybrid PSM/FDM method enables us to provide realistic simulation of regional wavefields that allow relatively high frequency propagation (~ 1 Hz) to a few hundred kilometers from the source. However it is still difficult to provide adequate resolution of surficial features

such as the presence of sedimentary basins, or a full treatment of oceanic structures including the strong contrast to the overlying fluid.

For many situations, such as the specific response to be expected in major population centres for hypothetical earthquakes, it is important to include the detailed structure of sedimentary basins. We can envisage linking the present style of hybrid computation scheme to an embedded finer scale model, so that e.g. a basin is illuminated by the wavefield generated in a regional model. Ideally we would need to consider the modification of the wavefield imposed by the finer scale structure, and to extract boundary conditions from the edges of the submodel to feed back into the regional calculation. Such a multigrid approach for high-resolution modelling has already been successfully employed with the 3-D finite-difference method (AOI and FUJIWARA, 1999). The use of such linked multi-scale calculation schemes for large-scale problems raises some computational difficulties, but may be possible to implement in certain styles of parallel architecture.

Acknowledgments

The collaboration of the authors has been supported by the Japanese Ministry of Education, Japan Society for the Promotion of Science and the Australian National University.

REFERENCES

AOI, S. and FUJIWARA, H. (1999), *3-D Finite-difference Method Using Discontinuous Grids*, Bull. Seismol. Soc. Am. *89*, 918–930.

FURUMURA, T. and KENNETT, B. L. N. (1998), *On the Nature of Regional Phases. III. The Influence of Crustal Heterogeneity on the Wavefield for Subduction Zone Earthquakes: the 1985 Michoacan and 1995, Copala, Guerrero, Mexico earthquakes*, Geophys. J. Int. *135*, 1060–1084.

FURUMURA, T. and KENNETT, B. L. N. (2001), *Variations in Regional Phase Propagation in the Area around Japan*, Bull. Seismol. Soc. Am. *91*, 667–682.

FURUMURA, T. and KOKETSU, K. (1998), *Specific Distribution of Ground Motion during the 1995 Kobe Earthquake and its Generation Mechanism*, Geophys. Res. Lett. *25*, 785–788.

FURUMURA, T., KOKETSU, K., and WEN, K.-L. (2001), *Parallel PSM/FDM Hybrid Simulation of Ground Motions from the 1999 Chi-Chi, Taiwan, Earthquake*, Pure Appl. Geophys., *159*, 2133–2146.

HASHIZUME, M., ITO, K., and YOSHII, T. (1981), *Crustal Structure of Southwestern Honshu, Japan and the Nature of the Mohorovicic Discontinuity*, Geophys. J. R. astr. Soc. *66*, 157–168.

KANAMORI, H. (1972), *Tectonic implications of the 1944 Toankai and the 1946 Nankaido Earthquakes*, Phys. Earth Planet. Inter. *5*, 129–139.

KAWASE, H. (1996), *The Cause of the Damage Belt in Kobe: "The Basin-edge Effect", Constructive Interference of the Direct S Wave with the Basin Induced/Diffracted Rayleigh Waves*, Seism. Res. Lett. *67*, 25–34.

KENNETT, B. L. N. (1989), *On the Nature of Regional Seismic Phases – I. Phase Representations for Pn, Pg, Sn, Lg*, Geophys. J. R. Astr. Soc. *98*, 447–456.

OLSEN, K. B. (2000), *Site Amplification in the Los Angeles Basin from Three-dimensional Modeling of Ground Motion*, Bull. Seismol. Sos. Am. *90*, S77–S94.

OLSEN, K. B. and ARCHULETA, R. J. (1996), *Three-dimensional Simulation of Earthquake on the Los Angeles Fault System*, Bull. Seismol. Soc. Am. *86*, 575–596.

SEKIGUCHI, H. and IWATA, T. (2000), *Rupture Process of the 2000 Tottori-Ken Seibu Earthquake Using Strong Ground Motion Data*, personal communication. (http://sms.dpri.kyoto-u.ac.jp/iwata/ttr_e.html).

SHIBUTANI, T., TADA, A., and HIRAHARA, K. (2000), *Crust and Slab Structure beneath Shikoku and the Surrounding Area Inferred from Receiver Function Analysis*, Abst. Seism. Soc. Japan 2000 Fall Meet. *B51*.

SHIMA, H. (1962), *On the Velocity of Lg Waves in Japan*, Quart. J. Seismol. *27*, 1–6 (in Japanese).

WALD, D. J. and GRAVES (1998), *The Seismic Response of the Los Angeles Basin, California*, Bull. Seismol. Soc. Am. *88*, 337–356.

YAGI, Y. and KIKUCHI, M. (2000), *Source Rupture Process of the Tottori-ken Seibu Earthquake of Oct. 6, 2000*, Personal communication. (http://wwweic.eri.u-tokyo.ac.jp/yuji/tottori/).

YOSHII, T., SASAKI, Y., TADA, T., OKADA, H., SHUZO, A., MURAMATU, I., HASHIZUME, M., and MORIYA, T. (1974), *The Third Kurayoshi Explosion and the Crustal Structure in Western Part of Japan*, J. Phys. Earth *22*, 109–121.

ZHAO, D. A., HORIUCHI, A., and HASEGAWA, A. (1992), *Seismic Velocity Structure of the Crust beneath the Japan Islands*, Tectonophysics *212*, 289–3–01.

ZHAO, D. and HASEGAWA, A. (1993), *P-wave Tomographic Imaging of the Crust and Upper Mantle beneath the Japan Islands*, J. Geophys. Res. *98*, 4333–4353.

(Received February 20, 2001, revised June 11, 2001, accepted June 25, 2001)